This is the **accepted version** of the journal article:

# New Squaramide-based Pt(II) Complexes, as Potential Oxygen-regulated Light-triggered Photocages

*Kevin Morales,[†] Katia G. Samper,[†] Quim Peña,[†] Jordi Hernando,[†] Julia Lorenzo,[††] Antonio Rodríguez-Diéguez,[‡] Mercè Capdevila,[†] Marta Figueredo,[†] Òscar Palacios\*[†] and Pau Bayón\*[†]*

[†] Departament de Química, Universitat Autònoma de Barcelona, 08193 Cerdanyola del Vallès, Spain.

[††] Departament de Bioquímica i Biologia Molecular, Institut de Biotecnologia i Biomedicina (IBB), Campus UAB, 08193 Cerdanyola del Vallès, Spain

[‡] Departamento de Química Inorgánica, Facultad de Ciencias, Universidad de Granada, 18071 Granada, Spain.

Two new squaramide-based platinum(II) complexes **C1** and **C2** have been synthesized and fully characterized. Their photoresponse has been assessed and is discussed. A remarkable enhancement in the DNA binding activity has been observed for both complexes, as a result of their irradiation. For **C2**, the release of Pt(II) provoked by its irradiation has been studied. The response of **C2** has been found to be regulated by the presence of oxygen. *In vitro*
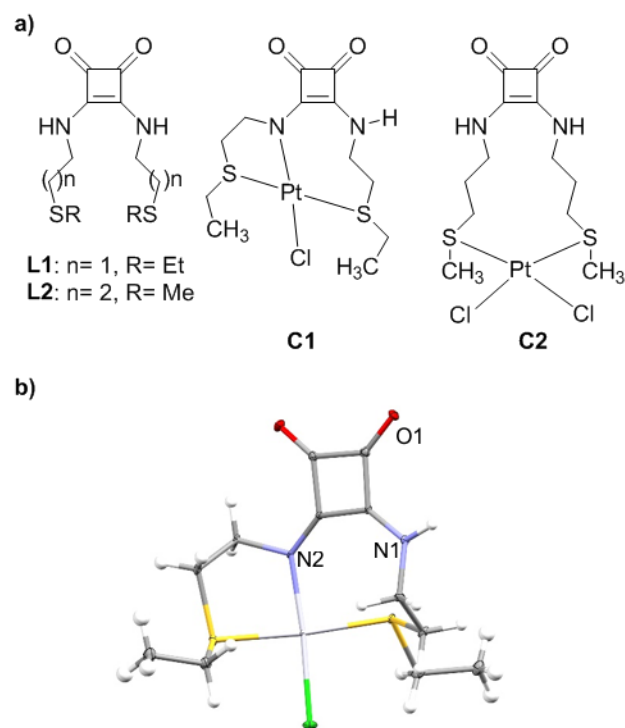
cytotoxicity tests show an enhancement in the activity of complex **C2** after irradiation selectively under hypoxic conditions. Resulting Pt(II) species have been isolated and characterized by various analytical methods revealing this type of squaramido-based complexes as proof of concept for new Pt(II) photocages.

**Introduction**

Around 50% of all patients who receive anticancer chemotherapy are treated with a platinum drug[1] despite their use is vastly disadvantaged by severe side-effects and development of resistance.[2] Due to these drawbacks, different approaches have been undertaken in order to overcome the inherent side effects of the drugs and to increase their selectivity.[3] Two of the most attractive alternatives emerged in the last years are: oxygen-dependent, photodynamic therapy (PDT)[4] and the so-called photoactivated chemotherapy (PACT),[4b,5] which overcomes the limitation of activity linked to oxygen in PDT.[4b,6] PACT is based on the use of species with low or negligible activity that can be structurally modified by means of an external photo-stimulus, therefore generating new active species against the tumor cells. The possibility to tune the structure, and hence the activity, allows to control when and, even more important, where the active drug performs its action.[4b] Interestingly, almost all the foregoing cases of PACT are based on the modification of the metal center and only scarce examples have considered the possibility to employ photocaging ligands in a Pt(II) complex to be used in light triggered release Pt(II) systems.[7] Here, we present a new approach to Pt(II) release, based on the use of Pt(II) complexes constituted by squaramido ligands responsible of their photoactivity.

Squaramide motifs are a class of interesting photoresponsive species that can be converted into their corresponding bisketenes (Scheme 1).[8] While this process reverts back thermally in non-nucleophilic solvents and under inert atmosphere, bisketenes can undergo irreversible reactions

with $H_2O$ in usual biological media, thereby preventing ring closure to recover the initial squaramide motif.[9]

**Scheme 1** Squaramide-bisketene interconversion in non-nucleophilic solvents and under inert atmosphere.



squaramide          bisketene

This photo-behavior prompted us to design a new class of squaramido type ligands for new Pt(II) photocages. These new ligands may stabilize the Pt(II) center, avoiding or substantially reducing its activity. Irradiation of these complexes would induce an irreversible photo-degradation process of the ligand in aqueous media,[9] consequently acting as a photocage, delivering Pt(II) in a more active form.

**Results and discussion**

First, ligands **L1** and **L2** were synthesized from dibutyl squarate and the corresponding aminothiols, following standard procedures for the synthesis of squaramides (Figure. 1a).[8] The structure of these two new compounds was confirmed by full characterization (see SI).

Once **L1** and **L2** were synthesized, the preparation of their corresponding Pt(II) complexes was addressed. To this aim, **L1** and **L2** were dissolved in an EtOH-$H_2O$ mixture and treated with $K_2PtCl_4$ under mild conditions to afford the corresponding Pt(II) complexes **C1** and **C2** as stable crystalline solids (Figure 1a).

**Figure 1.** (a) Ligands **L1**, **L2** and Pt(II) complexes **C1** and **C2**. (b) ORTEP drawing for **C1**.

Characterization of these two new complexes was accomplished (see SI). In the case of **C1** it was possible to determine its structure by single crystal X-ray diffraction analysis (Figure 1b, crystallographic data for this compound are compiled in the SI). Compound **C1** crystallizes in the monoclinic space group $P2_1/c$. The asymmetric unit consists of one platinum, one anionic ligand **L1** and one coordination chloride atom. In this case, platinum ion exhibits distorted square-planar $PtNS_2Cl$ geometry (Figure 1b) with the deprotonated N2 atom and the two sulphur atoms in *trans* positions. Pt-N and Pt-Cl distances have values of 2.016(2) and 2.3203(8) Å, respectively; whereas Pt-S distances are 2.2934(8) and 2.3050(9) Å. Each mononuclear complex connects with a neighbor unit by two strong hydrogen bonds, resulting in the formation of a dinuclear supramolecular entity (Figure S8). This hydrogen bond involves N1 and O1 atoms present in the structure. The bond distance has a value of 2.823(3) Å. The data reported allowed to confirm the chelating role of the ligand **L1**, occupying three binding sites and remaining only one chlorido

ligand, coming from the $K_2PtCl_4$ precursor. This coordination environment is directed by the highly rigid squaramide unit, which generates the distortion in the geometry of the metal center and hence the asymmetry observed for the whole complex. This fact would explain the observation of two clear differentiated sets of signals for the ethyl group in the $^1$H NMR spectrum of the complex **C1** (see SI), while only one set is observed for the free ligand **L1**. The differences in $^{13}$C NMR spectra of ligand **L1** and complex **C1** in the squaramide carbon region, from two up to four different signals confirm the change in symmetry after formation of the complex. The ESI-MS spectrum of compound **C1** was recorded (see SI). As expected, the main peaks obtained for **C1** correlate with the elucidated structure (519.03 Da) and its Na-adduct (541.01 Da).

Conversely, the analytical data of complex **C2** evidence no loss of symmetry in relation to the original free ligand **L2**. Thus, in the $^{13}$C NMR spectrum of **C2** a unique methyl group signal and only two signals in the squaramide region can be observed, as for the corresponding free ligand **L2** (see SI). The HRMS main peaks for **C2** correlate with the proposed species with loss of one and two chlorido ligands (519.02 and 482.05 Da, respectively) together with other peaks due to the formation of adducts with DMSO (597.04 Da and 560.07 Da). The lack of changes in the squaramide $^{13}$C NMR region after binding to the Pt(II) center in **C2**, together with data from UV-vis (*vide infra*) and elemental analysis, supports the assumption that coordination in **C2** is achieved only through the two thioether units without participation of the squaramide nitrogen atoms (Figure 1a).

The synthesis of these complexes has special relevance since there are scarce examples of metal complexes incorporating a squaramido motif in the structure of their ligands.[10] Above all, the case of the **C1** complex is particularly remarkable, since there is a direct participation of the nitrogen

atom in the coordination sphere of the metal. To the best of our knowledge, **C1** is the first metal complex where the squaramide unit is directly coordinated to a platinum center .[10f]

Once the ligands and complexes were characterized, the next endeavor was studying the photo-behavior of these species. Figure 2 displays the UV-vis absorption spectra of **L1**, **L2** and their corresponding Pt(II) complexes **C1** and **C2** in a 98:2 water:DMSO mixture. As already reported for other squaramide derivatives,[8] **L1** and **L2** show similar and strong absorption in the UV region (maxima at 291 and 294 nm, respectively), which are differently affected by metal complexation. In the case of **C1**, the UV absorption band bathochromically shifts to 317 nm and an additional, less intense band appears at *ca.* 400 nm (Figure 2a). Based on the structure resolved for this complex by X-ray crystallography, we ascribe this behavior to the direct participation of the nitrogen atoms of the squaramide unit in the complexation to the metal center, thus altering the optical properties of the chromophore. On the contrary, negligible spectral changes were observed between ligand **L2** and its complex **C2** ($\lambda_{abs,max}$ = 294 nm) (Figure 2b). This fact reinforces the structure proposed for this complex in Figure 1a, where coordination to the metal ion takes place via the pending thioether groups and does not directly involve the squaramide motif.
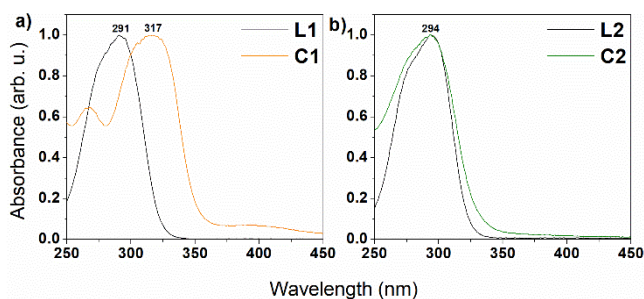


**Figure 2.** Comparative UV-vis absorption spectra in 98:2 water:DMSO of (a) ligand **L1** and its corresponding Pt(II) complex **C1** and (b) **L2** and **C2**.

The photoactive behavior of complexes **C1** and **C2**, as well as that of their constituting ligands **L1** and **L2**, was furtherly investigated by both time-resolved and steady-state electronic

spectroscopy in aqueous media. Due to the high rates reported for bisketene→squaramide thermal back-isomerization,[8] the light-induced interconversion between these two states was first explored by transient absorption spectroscopy. Upon pulsed irradiation at 266 nm, negative transient absorption signals (ΔAbs) were mainly recorded in the UV region (see SI), a situation already reported for squaramides and ascribed to their photoisomerization to the less absorbing bisketene product.[8] As previously discussed, such a light-generated compound can either return back thermally to the initial squaramide state on the sub-second scale or undergo irreversible reactions with the surrounding media that would prevent back-isomerization (e.g. with water molecules).[9] Since no time decay of the negative transient absorption signals was recorded, the latter appears to be the major evolution pathway under our experimental conditions, i.e. quantitative degradation of the light-generated bisketene derivatives. Importantly, this behavior was encountered for both ligands **L1-L2** and complexes **C1-C2**, thus demonstrating that the photoactivity of the free ligands is not suppressed upon Pt(II) complexation and, consequently, enabling our strategy towards light-responsive squaramide-based Pt(II) complexes.

To further investigate the irreversible photodegradation of the squaramide chromophore in ligands **L1** and **L2** and their corresponding complexes **C1** and **C2**, the variation of their steady-state electronic absorption spectra upon irradiation with UV light was monitored (Figure 3). In all the cases, similar results were observed. When subjected to prolonged illumination, a continuous decrease of the intense squaramide absorption bands at *ca.* 290 nm (**L1**, **L2** and **C2**) and 317 nm (**C1**) was registered, while an absorption shoulder at longer wavelengths was developed. These changes occurred at lower rates for the complexes than for the free ligands, thus hinting at reduced photoactivity of the squaramide unit upon complexation, as already anticipated by the lower ΔAbs signals measured for **C1** and **C2**. In spite of this, subsequent recovery of the squaramide spectral

features in the dark was observed for none of the compounds, which confirms that both free ligands and complexes undergo extensive irreversible photodegradation.
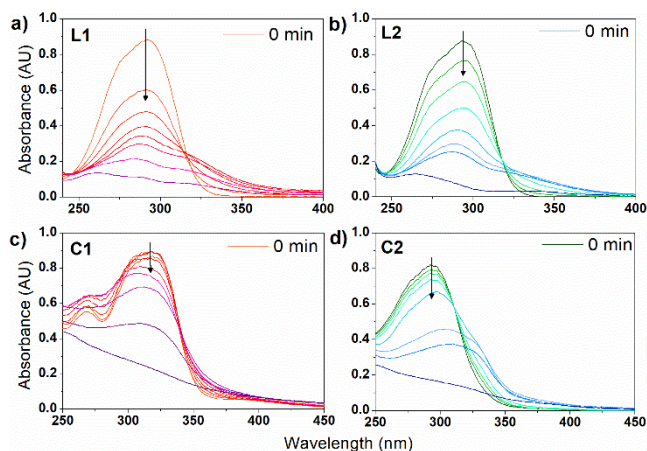


**Figure 3.** Time evolution of the UV-vis absorption spectra in water:DMSO, (98:2) of (a) ligand **L1**, (b) **L2**, (c) complex **C1** and (d) **C2**.

With **C1**, **C2** and their corresponding irradiation products **C1'** and **C2'** in hands, we proceeded to assess their interaction with calf thymus DNA (ct-DNA).[11,12] The CD spectrum of ct-DNA exhibits a characteristic positive band at 275 nm due to base stacking and a negative band at 248 nm due to helicity of B-DNA.[13] Aliquots of ct-DNA samples (100 µM) were titrated with stock solutions of **C1**, **C2**, **C1'** or **C2'**. The CD spectra, corresponding to the incubation at different molar ratios, were recorded under the same conditions (Figure 4). For **C1** and **C2** no significant changes were observed, indicating that these complexes would not modify apparently the DNA structure after incubation (Figure 4a and 4c). However, both **C1'** and **C2'** provoke changes in the CD signals of ct-DNA, showing a slight decrease of the positive band at 270 nm upon increasing complex concentration (Figure 4b and 4d). These changes of the B-type CD spectrum seems to indicate that **C1'** leads to some conformational changes as conversion to a more C-like structure in DNA molecule.[12b] Interestingly, incubation with **C2'** shows a more significant decrease in the

intensity of both, negative and positive, ct-DNA bands. These two concomitant results indicate a destabilization of base-stacking and loss of right-handed helicity and, therefore, suggest modifications in the secondary structure of DNA promoted by **C2'**.

When considering all these results together, it points out that in both **C1** and **C2** the ligand exerts sufficient hindrance on the Pt(II) center as to impair the reactivity of Pt moiety with ct-DNA, whereas their photo-conversion to **C1'** and **C2'**, provoke an increase of the reactivity, being **C2'** the most active among them.
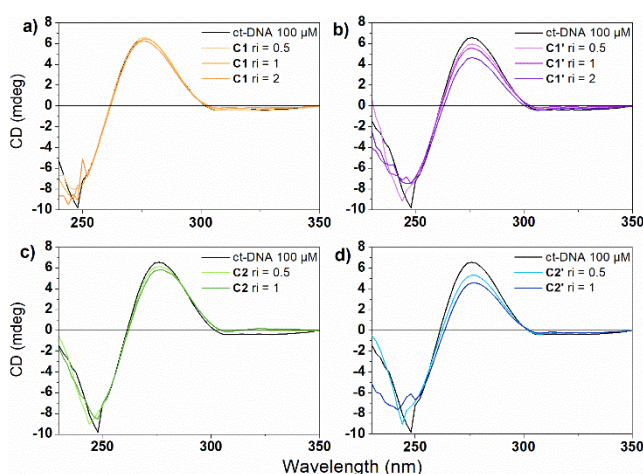


**Figure 4.** CD spectra of ct-DNA and ct-DNA incubated with (a) **C1**, (b) **C1'**, (c) **C2**, and (d) **C2'** at different molar ratio (ri).

At this point, it was reasonable to perform a comparative cell viability test in order to consider the potential application of **C1** and **C2** as light-triggered Pt(II) delivering systems. To this aim, complexes **C1**, **C2**, **C1'** and **C2'** were screened for their in vitro antiproliferative activity against cisplatin resistant human adenocarcinoma HeLa cells. Complex **C1** presents a moderate cytotoxicity (IC$_{50}$= 74±18 µM), while **C1´** turned out to be too insoluble in the conditions required for cell viability screening. Then, it was encountered that **C2** did not show any cytotoxic effect up to the 200 µM concentration. Gratifyingly, in this case, irradiated **C2'** resulted clearly soluble after

incubation making reliable its assessment. At this point, the assay was planned in both, presence and absence of oxygen, as hypoxic conditions are encountered in tumor tissues.[4b,14] Interestingly, when **C2'** was produced under normoxic conditions (**C2'N**) no relevant *in vitro* antitumor activity was observed. Unexpectedly, when **C2'** was generated under hypoxic conditions (**C2'H**) a remarkable enhancement of reactivity was observed ($IC_{50}$= 69±8 µM).

In the light of these last results, we concentrated our efforts on the investigation of the apparently oxygen controlled process occurring when complex **C2** was irradiated. First, the corresponding ligand **L2** was irradiated in both normoxic (**L2'N**) and hypoxic (**L2'H**) conditions. Analysis of the resulting irradiation crude product under normoxic conditions revealed the presence of aminium sulfide **S-H+** and its corresponding sulfoxide **SO-H+**, whereas the analysis in hypoxic conditions showed to be very selective towards sulfide, **S-H+**, production (Scheme 2).

**Scheme 2.** Oxygen controlled product selectivity in the irradiation of **C2**.
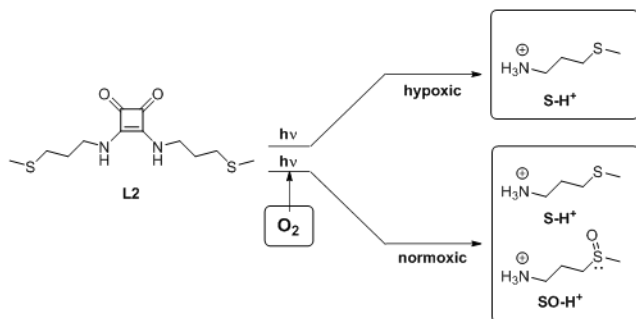


In order to confirm these results, samples of **S-H+** and **SO-H+** were prepared from commercial 2-(methylthio)propan-1-amine. ^{1}H NMR spectra of these products were compared with the crude products of **L2** irradiation in both normoxic, **L2'N**, and hypoxic conditions, **L2'H**. In the case of normoxic irradiation, ^{1}H NMR analysis revealed the presence of both **S-H+** and **SO-H+** in *ca.* 1:1 ratio and, gratifyingly, hypoxic irradiation produced selectively protonated sulfide **S-H+** (Figure 5).[15]
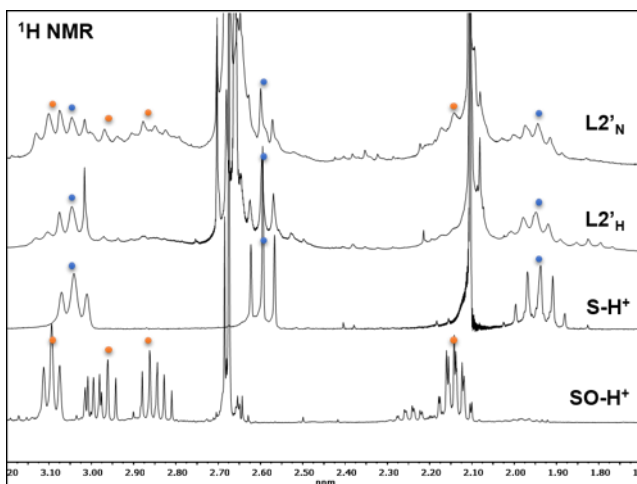
**Figure 5.** Comparison of the significant signals in $^1$H NMR spectra of **L2'$_N$** and **L2´$_H$** with sulfur **S-H$^+$** and sulfoxide **SO-H$^+$**.

Once the influence of oxygen in the irradiation process of squaramide **L2** was demonstrated, the corresponding Pt(II) complex was also studied.

Irradiation of **C2** in the presence of oxygen, **C2'$_N$**, revealed the presence of **S-H$^+$** and **SO-H$^+$** in a *ca.* 1:1.25 ratio. Hypoxic irradiation resulted in **C2'$_H$** where **S-H$^+$** was detected almost exclusively, though some traces of **SO-H$^+$** were present as detected by NMR analysis (Figure 6).
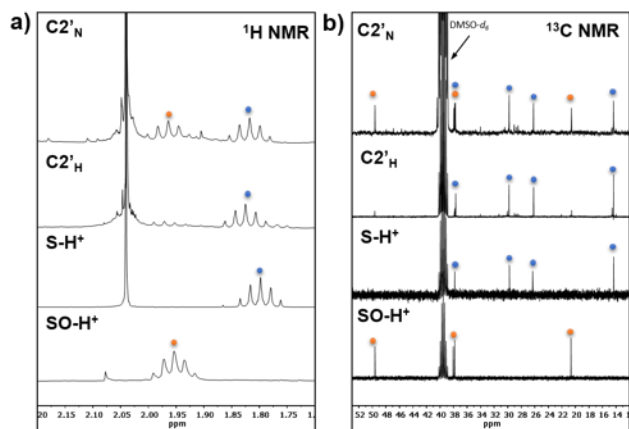


**Figure 6.** Comparison of the significant signals in $^1$H NMR and $^{13}$C NMR spectra of **C2'$_N$** and **C2´$_H$** with sulfur **S-H$^+$** and **SO-H$^+$**.

Irradiation of **C2** was monitored by high resolution mass spectroscopy (HRMS). In normoxic conditions, the irradiatiated mixture presented initially a set of peaks at 428, 443 and 473 Da evolving in time to mainly a 443 Da peak, **C2´N**. This is consistent with a complex in which both ligands, sulfide, **S-H⁺**, and sulfoxide, **SO-H⁺**, participate as anticipated by NMR (see SI). Nevertheless, an accurate interpretation of its structure has not been possible probably due to the degradation of the samples under the analysis conditions. HRMS analysis of the hypoxic irradiation mixture, **C2'H**, clearly showed a 414 Da peak (see SI). Consequently, the structure for **C2'H** is suggested, where 3-(methylthio)propan-1-amine, coming from the initial squaramide unit, acts as a ligand (Figure 7a). In order to confirm this structure, the corresponding dichlorido complex, **C2s**, was synthesized from commercially available materials allowing to its full characterization (see SI). The structure of this new complex, has been elucidated by X-ray diffraction analysis (Figure 7b).[16] Confirming the already proposed Pt environment: Platinum ion exhibits distorted square-planar PtNSCl₂ geometry with the neutral N atom form –NH₂ and one sulfur atom together with 2 chlorido ligands in *cis* configuration. In addition, when the synthesized complex was analyzed by HRMS, the recorded data allowed to observe the complete coincidence of mass pattern with **C2'H**. In both cases the main peak corresponds to 414 Da suggesting that in the complex **C2s** one chlorido ligand has been replaced by a DMSO molecule. In conclusion, Figure 7a shows the structure suggested for **C2'H** derivate from the active Pt(II) complex, **C2s** (Figure 7b) released from the photocage **C2**.
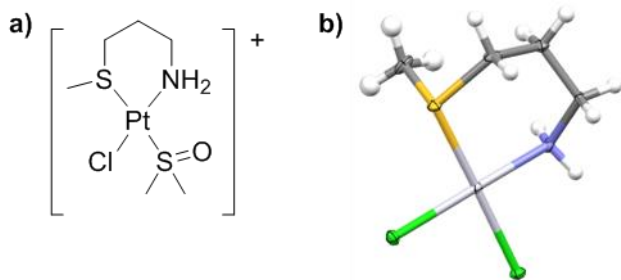
**Figure 7:** (a) Suggested structure for **C2'$_H$**. (b) ORTEP drawing for **C2s**.

Remarkably, this is the first example of the use of a squaramide type photocage as a platinum release device and, more interestingly, it has been demonstrated the dependence on oxygen in the manner platinum is released i.e. the antiproliferative activity.[17] It may be possible in the future to exploit these qualities for the application in various fields, for instance, hypoxia targeting agents.

In summary, the synthesis of two new stable squaramide-based Pt(II)-complexes has been achieved and their full characterization presented. Complex **C1** is the first example of a platinum complex directly coordinated to a squaramide motif. The photochemical behavior of **C1** and **C2** has been investigated. In particular for **C2**, photo-degradation has been studied in normoxic and hypoxic conditions. Regarding this fact, **C2** showed to be highly sensitive to oxygen as two different results can be produced depending on irradiation conditions (normoxic and hypoxic media produce **C2'$_N$** and **C2'$_H$** respectively). Structural elucidation of these irradiation products has been discussed. In addition, **C1** and **C2** showed an enhancement in their ability to interact with DNA by means of irradiation. This has been observed when comparing the effect in CD spectra of DNA incubated with **C1**, **C2** complexes and their corresponding photochemical products. When all complexes were submitted to HeLa cell viability, **C1** showed moderated IC$_{50}$= 74±18 while its irradiated form could not be assessed due to solubility issues. More interestingly, **C2**, has shown to be inactive as its normoxic irradiation product **C2'$_N$** but, gratefully, under hypoxic conditions, **C2'$_H$** revealed remarkable enhancement of the antiproliferative activity IC$_{50}$= 69±8 against HeLa, what is in the same range of well-established carboplatin IC$_{50}$=38.7.[18]

The present work aims to be a proof of concept for a new class of photocages based on first described squaramide Pt(II) complexes. Furthermore, oxygen has been demonstrated to exert good

control on the nature of the released species and therefore in the activity against HeLa cells. These promising results encourage us to the preparation and study of new complexes, which will hopefully contribute to the design of new alternatives in PACT, particularly leading to oxygen tension dependent reactivity.

### Experimental section

**Materials.** $K_2PtCl_4$ was purchased from Strem Chemicals. Different organic reagents, used for ligands synthesis, were purchased from Sigma-Aldrich or Alfa Aesar. All solvents were dried before use.

**Synthesis.** *3,4-bis{[2-(ethylsulfanyl)ethyl]amino}cyclobut-3-ene-1,2-dione* (**L1**). To a solution of 3,4-dibutoxy-3-cyclobutene-1,2-dione (302 μL, 1.40 mmol) in diethyl ether (5 mL) was added 2-(ethylthio)ethylamine (0.62 mL, 5.58 mmol). The mixture was stirred at room temperature for 1 h. After this time, a white solid precipitated. After filtering out the solvent, the white solid was carefully washed with diethyl ether to afford the product as a white powder (373 mg, 1.29 mmol, 92%).

$^1$H NMR (400 MHz, DMSO-$d_6$, 320 K): $\delta$ = 7.60 (br, 2H), 3.72-3.62 (m, 4H), 2.69 (t, $J$ = 6.7 Hz, 4H), 2.55 (q, $J$ = 7.4 Hz, 4H), 1.18 (t, $J$ = 7.4 Hz, 6H). $^{13}$C-NMR (100 MHz, DMSO-$d_6$, 320 K): $\delta$ = 182.4, 167.5, 42.8, 32.0, 24.7, 14.6. HRMS (ESI+): calculated for [$C_{12}H_{20}N_2O_2S_2$]: 289.1039 [M+H$^+$]; found 289.1034. UV (DMSO) $\lambda_{max}$, nm ($\varepsilon$, M$^{-1}$ cm$^{-1}$): 293 (3.07x10$^4$). IR (cm$^{-1}$): 3166, 2955, 2922, 1804, 1633, 1573, 1482, 1433, 1351, 1298, 1268, 1223, 1111, 1058, 993, 970, 932, 860.

*3,4-bis{[3-(methylsulfanyl)propyl]amino}cyclobut-3-ene-1,2-dione* (**L2**). To a solution of 3,4-dibutoxy-3-cyclobutene-1,2-dione (302 μL, 1.40 mmol) in diethyl ether (5 mL) was added 3-(methylthio)propylamine (0.63 mL, 5.62 mmol). The mixture was stirred at room temperature for

1 h. After this time, a white solid precipitated. After filtering out the solvent, the white solid was carefully washed with diethyl ether to afford the product as a white powder (366 mg, 1.27 mmol, 91%).

$^1$H-NMR (400 MHz, DMSO-$d_6$, 380 K): $\delta$ = 7.12 (br, 2H), 3.63-3.56 (m, 4H), 2.54 (t, $J$ = 7.0 Hz, 4H), 2.08 (s, 6H), 1.85 (quint, $J$ = 7.0 Hz, 4H). $^{13}$C-NMR (100 MHz, DMSO-$d_6$, 320 K): $\delta$ = 182.3, 167.7, 42.2, 30.1, 30, 14.4. HRMS (ESI+): calculated for [$C_{12}H_{20}N_2O_2S_2$]: 289.1039 [M+H$^+$]; found 289.1035. UV (DMSO) $\lambda_{max}$, nm ($\varepsilon$, M$^{-1}$ cm$^{-1}$): 294 (4.75x10$^4$). IR (cm$^{-1}$): 3158, 2948, 2915, 1799, 1635, 1574, 1479, 1430, 1345, 1274, 1185, 1109, 1071, 1014, 959, 903, 872.

*Pt(C$_{12}$H$_{19}$N$_2$O$_2$S$_2$)Cl* (**C1**). **L1** (42.1 mg, 0.15 mmol) and potassium tetrachloroplatinate (61.8 mg, 0.15 mmol) were suspended in a mixture of ethanol and water (1:1, 8 mL). The suspension was stirred at room temperature under inert atmosphere for 4 h. After this time, a yellow solid precipitates. After filtering out the solvent the yellow solid was washed with hot ethanol and diethyl ether to afford the product as a yellow powder. The powder was recrystallized in dimethyl sulfoxide to afford orange crystals (35 mg, 0.07 mmol, 45%).

$^1$H-NMR (400 MHz, DMSO-$d_6$, 360 K): $\delta$ = 7.42-7.22 (m), 3.20-3.08 (m), 3.04 (s), 2.78-2.69 (m), 2.63-2.53 (m), 1.45 (t, $J$ = 7.3 Hz), 1.38 (t, $J$ = 7.3 Hz), 1.32 (t, $J$ = 7.3 Hz), 1.22 (td, $J$ = 7.3, 2.1 Hz). $^{13}$C-NMR (100 MHz, DMSO-$d_6$, 360 K): $\delta$ = 185.6, 179.6, 172.8, 166.3, 44.2, 42.8, 35.9, 34.8, 31.9, 27.5, 24.6, 14.3, 12.9, 11.3. HRMS (ESI+): calculated for [$C_{12}H_{19}N_2O_2S_2PtCl$]: 519.0285 [M+H]$^+$, 541.0105 [M+Na]$^+$; found 519.0296 [M+H]$^+$, 541.0105 [M+Na]$^+$. EA calculated for $C_{12}H_{19}N_2O_2S_2PtCl$ (%): C 27.83, H 3.70, N 5.41, S 12.38; found: C 28.05, H 3.72, N 5.25, S 11.76. UV (DMSO) $\lambda_{max}$, nm ($\varepsilon$, M$^{-1}$ cm$^{-1}$): 279 nm (1.75x10$^4$); 318 nm (1.58x10$^4$); 334 nm (1.64x10$^4$); 427 nm (9.73x10$^2$). IR (cm$^{-1}$): 3199, 3058, 2967, 2874, 2343, 1774, 1634, 1560,

1534, 1466, 1449, 1410, 1347, 1336, 1286, 1275, 1259, 1220, 1169, 1153, 1101, 1078, 1052, 1020, 1009, 990, 969, 957, 873, 860, 789, 776, 729.

*Pt($C_{12}H_{20}N_2O_2S_2$)Cl₂* (**C2**). **L2** (52.7 mg, 0.18 mmol) and potassium tetrachloroplatinate (76.1 mg, 0.18 mmol) were suspended in a mixture of ethanol and water (1:1, 8 mL). The suspension was stirred at room temperature under inert atmosphere for 6 h. After this time, a light yellow solid precipitates. After filtering out the solvent the solid was washed with hot ethanol and diethyl ether to afford the product as a yellow powder. The powder was recrystallized in dimethyl sulfoxide to afford yellow crystals (76 mg, 0.14 mmol, 78%).

$^1$H-NMR (250 MHz, DMSO-$d_6$): $\delta$ = 7.70-7.35 (m), 3.68-3.50 (m), 3.29 (br), 2.58-2.52 (m), 2.05 (s), 1.79 (quint, $J$ = 7.4 Hz). $^{13}$C-NMR (100 MHz, DMSO-$d_6$, 360 K): $\delta$ = 182.3, 167.7, 42.1, 29.9, 29.9, 14.2. HRMS (ESI+): calculated for [$C_{12}H_{20}N_2O_2S_2PtCl_2$]: 482.0531 [M-2Cl-H]$^+$, 519.0285 [M-Cl]$^+$, 560,0671 [M-2Cl-H+DMSO]$^+$, 597,0424 [M-Cl+DMSO]$^+$; found 482.0511[M-2Cl-H]$^+$, 519.0244 [M-Cl]$^+$, 560,0654 [M-2Cl-H+DMSO]$^+$, 597,0417 [M-Cl+DMSO]$^+$. EA calculated for $C_{12}H_{20}N_2O_2S_2PtCl_2$ (%): C 26.00, H 3.64, N 5.05, S 11.57; found: C 25.80, H 3.83, N 4.48, S 10.98. UV (DMSO) $\lambda_{max}$, nm ($\varepsilon$, M$^{-1}$ cm$^{-1}$): 293 (3.32x10$^4$). IR (cm$^{-1}$): 3247, 3002, 2918, 2360, 2341, 1796, 1663, 1585, 1529, 1482, 1416, 1348, 1314, 1273, 1227, 1127, 1017, 955, 817.

*Pt($C_4H_{11}NS$)Cl₂* (**C2s**). 3-(Methylthio)propan-1-amine (98 µL, 0.89 mmol) and potassium tetrachloroplatinate (340.2 mg, 0.82 mmol) were suspended in a mixture of methanol and water (1:1, 18 ml). The suspension was stirred at room temperature under inert atmosphere for 1.5 h. After this time, a light pink solid precipitates. After filtering out the solvent the solid was washed with water, ethanol and diethyl ether to afford the product as a pink powder. (267 mg, 0.72 mmol, 88%). This powder was recrystallized in dimethyl sulfoxide to afford yellow crystals that were

submitted to XRD analysis. The same crystalline solid was diluted in DMSO-$d_6$ for NMR analysis. In this way, DMSO- Cl exchange was unavoidable giving a mixture.

$^1$H-NMR (400 MHz, DMSO-$d_6$) (mixture of DMSO/Cl complexes): $\delta$ = 6.00-5.90 (m), 5.80-5.70 (m), 5.30-5.00 (br), 3.32 (s), 3.03-2.97 (m), 2.85-2.76 (m), 2.73 (s), 2.72-2.58 (m), 2.54 (s), 2.48 (s), 1.99 (quint, $J$ = 6.0 Hz). $^{13}$C-NMR (100 MHz, DMSO-$d_6$) (mixture of DMSO/Cl complexes): $\delta$ = 48.6 (Cl), 41.6 (DMSO), 30.9 (DMSO), 30.6 (Cl), 24.0 (DMSO), 23.1 (Cl), 20.6 (DMSO), 20.4 (Cl). HRMS (ESI+): calculated for $[C_4H_{11}NSPtCl_2]$: 414.0068 $[M-Cl+DMSO]^+$; found 414.0072. EA calculated for $C_4H_{11}NSPtCl_2$ (%): C 12.94, H 2.99, N 3.77, S 8.64; found: C 13.15, H 3.02, N 3.69, S 8.62.

*3-(Methylsufinyl)propan-1-amine* (**SO**).[19] 15 µl of a 30% $H_2O_2$ solution was added to a methanol solution (2.5 mL) containing 3-(methylthio)propan-1-amine (251 µL, 2.29 mmol), 15 µl isopropyl alcohol and 15 µL of concentrated $H_2SO_4$. The solution was stirred at room temperature for 40 h. After this time, 2.5 mL of $H_2O$ and 2.5 mL of brine were added. The reaction mixture was extracted with 4x25 mL $CH_2Cl_2$. The combined organic phases were dried over anhydrous $Na_2SO_4$ and concentrated under vacuum to give an oily residue. The crude product was used without further purification.

$^1$H-NMR (400 MHz, CD$_3$OD): $\delta$ = 2.94-2.75 (m, 4H), 2.65 (s, 3H), 1.94-1.85 (m, 2H). $^{13}$C-NMR (100 MHz, CD$_3$OD): $\delta$ = 52.3, 41.4, 38.2, 26.8.

**X-ray Structure Determination.** Prismatic crystal for **C1** and **C2s** were mounted on a glass fiber and used for data collection on a Bruker D8 Venture with Photon detector equipped with graphite monochromated MoKα radiation (λ=0.71073 Å). The data reduction was performed with the APEX2[20] software and corrected for absorption using SADABS.[21] Crystal structures were solved by direct methods using the SIR97 program[22] and refined by full-matrix least-squares on

$F^2$ including all reflections using anisotropic displacement parameters by means of the WINGX crystallographic package.[23] For compound **C1** hydrogen atom bonded to N1 atom has been located in a Fourier synthesis, included and refined as riding on bonded atom. Generally, anisotropic temperature factors were assigned to all atoms except for C9 and hydrogen atoms, which are riding their parent atoms with an isotropic temperature factor arbitrarily chosen as 1.2 times that of the respective parent.

Details of these structure determinations and refinements of compounds are summarized in Table S1. Crystallographic data (excluding structure factors) for the structures reported in this paper have been deposited with the Cambridge Crystallographic Data Center as supplementary publication numbers CCDC 1535610 and 1838579. Copies of the data can be obtained free of charge on application to the Director, CCDC, 12 Union Road, Cambridge, CB2 1EZ, U.K. (Fax: +44-1223-335033; e-mail: deposit@ccdc.cam.ac.uk or http://www.ccdc.cam.ac.uk).

**Photochemical characterization.** All spectroscopic and photochemical experiments were carried out in 98:2 mixtures of MilliQ water and HPLC quality DMSO, under air atmosphere and with concentrations *ca.* 15-50 μM for all the compounds under investigation. Steady-state UV-vis absorption measurements were recorded on a HP 8453 spectrophotometer. Transient absorption measurements were registered in a ns laser flash-photolysis system (LKII, Applied Photophysics) equipped with a Nd:YAG laser (Brilliant, Quantel, 4th harmonic, λ=266 nm, power=4.5 mJ/pulse) as a pump source, a Xe lamp as a probe source and a photomultiplier tube (Hamamatsu) coupled to a spectrograph as a detector. Continuous irradiation of the solutions of photoactive compounds was performed using a UV lamp (Vilber-Lormat, λ=312 nm, 6 W) or a high-pressure mercury

lamp contained in a water-cooled, Pyrex immersion well (125 W) (see SI for more detailed information).

**Circular Dichroism Spectroscopy.** CD spectroscopy was performed using a spectropolarimeter with 1 cm path-length cuvettes. Measurements were carried out at a constant temperature of 20 ºC. CD spectra were measured in 10 mM TRIS-HCl buffer (pH 7.24). Calf thymus DNA concentration was 100 µM. Different samples with increasing amount of the Pt complex to study (0, 50, 100 and 200 µM) were incubated at 37 ºC for 24 h before spectra were recorded in the range of 200-350 nm. Complexes were added from stock 2% DMSO water solutions.

**Cell Viability Assays.** Human cancer cells (HeLa) were obtained from American Type Culture Collection (ATCC, Manassas, VA, USA) and were routinely cultured in MEM (modified Eagle's medium) alpha (Invitrogen) containing 10% heat-inactivated fetal bovine serum (FBS) at 37 ºC in a humidified $CO_2$ atmosphere. The cytotoxicity of each complex was evaluated using PrestoBlue Cell Reagent (Life Technologies) assay. Stock solutions for complexes **C1** and **C2** were freshly prepared in DMSO. **C2'** stock samples were obtained by total irradiation (at 312 nm) of DMSO-$H_2O$ solutions under normoxic (air atmosphere) or hypoxic ($N_2$ degassed by bubbling stream through the septum cap of the sealed cuvette for 15 min prior to irradiation) conditions for **C2'$_N$** and **C2'$_H$**, respectively. All working concentrations were prepared in MEM alpha medium for working concentrations (maximum 0.2% DMSO in biological experiments). Cells were plated in 96 well plates at a density of $5x10^3$ cells/well in 100 µl of culture medium and were allowed to grown overnight. After this time, cells were treated with different concentrations (0, 10, 25, 50, 100 or 200 µM) of each complex during 72h and then 10 µL of PrestoBlue® were added following the standard protocol. After 3 h incubation, fluorescence (at 590 nm) was measured by a microplate

reader (Victor3). The relative cell viability (%) for each sample related to the control well was calculated. Each sample was tested in triplicate.

ASSOCIATED CONTENT

**Supporting Information**.

The following files are available free of charge.

Sample irradiation procedures, photochemical characterization of ligands and complexes, $IC_{50}$, plot, spectra obtained by HRMS, ^{1}H NMR and ^{13}C NMR. (PDF)

Crystallographic data and ORTEP illustration of **C1** and **C2$_s$**. (PDF)

**Accession codes**

CCDC number for **C1** 1535610 and **C2$_s$** 1838579 contain the supplementary crystallographic data for this paper. These data can be obtained free of charge via www.ccdc.cam.ac.uk/data_request/cif or by emailing data_request@ccdc.cam.ac.uk , or by contacting The Cambridge Crystallographic Data Centre, 12 Union Road, Cambridge CB2 1EZ, UK; fax: +44 1223 336033.

AUTHOR INFORMATION

**Corresponding Author**

*E-mail: pau.bayon@uab.cat

*E-mail: oscar.palacios@uab.cat

ORCID

Pau Bayón: 0000-0002-3064-8866

Kevin Morales: 0000-0001-6096-7174

Òscar Palacios: 0000-0002-2987-7303

**Notes**

REFERENCES

(1) (a) Johnstone, T. C.; Park, G. Y.; Lippard, S. J. Understanding and improving platinum anticancer drugs–phenanthriplatin. *Anticancer Res.* **2014**, *34*, 471-476. (b) For a recent comprehensive review on platinum therapies: Bergamo, A.; Dyson, P. J.; Sava G. The mechanism of tumour cell death by metal-based anticancer drugs is not only a matter of DNA interactions. *Coord. Chem. Rev.* **2018**, *360*, 17–33.

(2) (a) Jamieson, E. R.; Lippard, S. J. Structure, recognition, and processing of cisplatin-DNA adducts. *Chem. Rev.* **1999**, *99*, 2467-2498. (b) Lloyd, K. The resurgence of platinum-based cancer chemotherapy. *Nature Rev. Cancer* **2007**, *7*, 573-587.

(3) (a) Shaili, E. Platinum anticancer drugs and photochemotherapeutic agents: recent advances and future developments. *Sci. Prog.* **2014**, *97*, 20-40, and references in. (b) Szymanski, W.; Ourailidou, M. E.; Velema, W. A.; Dekker, F. J.; Feringa, B. L. Light-controlled histone

deacetylase (hdac) inhibitors: towards photopharmacological chemotherapy. *Chem. Eur. J.* **2015**, *21*, 16517-16524.

(4) (a) Farrer, N. J.; Sadler, P. J. Photochemotherapy: targeted activation of metal anticancer complexes. *Aust. J. Chem.* **2008**, *61*, 669-674, and references in. (b) Mitra, K. Platinum complexes as light promoted anticancer agents: a redefined strategy for controlled activation. *Dalton Trans.* **2016**, *45*, 19157-19171, and references in. (c) Wang, Y.; Xie, Y.; Li, J.; Peng, Z-H.; Sheinin, Y.; Zhou, J; Oupický, D. Tumor-penetrating nanoparticles for enhanced anticancer activity of combined photodynamic and hypoxia-activated therapy. *ACS Nano* **2017**, *11*, 2227-2238.

(5) Farrer, N. J.; Salassa, L.; Sadler, P. J. Metal anticancer compounds. *Dalton Trans.* **2009,** 10690-10701, and references in.

(6) Chen, Y.; Lei, W.; Jiang, G.; Hou, Y.; Li, C.; Zhang, B.; Zhou, Q.; Wang, X. Fusion of photodynamic therapy and photoactivated chemotherapy: a novel Ru(II) arene complex with dual activities of photobinding and photocleavage toward DNA. *Dalton Trans.* **2014**, *43*, 15375-15384, and references in.

(7) (a) Ciesienski, K. L.; Hyman, L. H.; Yang, D. T.; Haas, K. L.; Dickens, M. G.; Holbrook, R. J.; Franz, K. J. A Photo-caged platinum(II) complex that increases cytotoxicity upon light activation. *Eur. J. Inorg. Chem.* **2010**, 2224-2228. (b) Presa, A.; Brissos, R. F.; Caballero, A. B.; Borilovic, I.; Korrodi-Gregório, L.; Pérez-Tomás, R.; Roubeau, O.; Gamez, P. Photoswitching the cytotoxic properties of platinum(II) compounds. *Angew. Chem. Int. Ed.* **2015**, *54*, 4561-65. (c) Presa, A.; Vázquez, G.; Barrios, L. A.; Roubeau, O.; Korrodi-Gregório, L.; Pérez-Tomás, R.; Gamez, P. Photoactivation of the cytotoxic properties of platinum(II) complexes through ligand photoswitching. *Inorg. Chem.* **2018**, *57*, 4009-4022.

(8) Fu, N.; Allen, A. D.; Kobayashi, S.; Tidwell, T. T.; Vukovic, S.; Arumugam, S.; Popik, V. V.; Mishima, M. Amino substituted bisketenes: generation, structure, and reactivity. *J. Org. Chem*. **2007**, *72*, 1951-1956.

(9) (a) Nguyen, M. T.; Raspoet, G. The hydration mechanism of ketene:15 years later. *Can. J. Chem*. **1999**, *77*, 817- 829. (b) Hao, X.; Liu, R.; Lusztyk, J.; Ma, M.; McAllister, M. A.; Rubin, Y.; Sung, K.; Tidwell, T. T.; Wagner, B. D. Generation of 1,2-bisketenes from cyclobutene-1,2-diones by flash photolysis and ring closure kinetics. *J. Am. Chem. Soc.* **1997**, *119,* 12125-12130.

(10) For examples of squaramide ligand complexes see: (a) Fabre, P-L.;  Galibert, A. M.; Soula, B.; Dahan, F.; Castan, P. Complexation of 3,4-bis(cyanamido)cyclobutane-1,2-dione dianion with copper. Crystal structures and spectroscopic data of copper-(I) and -(II) complexes. *J. Chem. Soc Dalton Trans*. **2001**, 1529 –1536. (b) Cortadellas, O.; Galibert, A. M.; Soula, B.; Donnadieu, B.; Fabre, P-L. Palladium(II) complexes obtained from 3,4 bis(cyanamido)cyclobutane-1,2-dione dianion. *Inorg. Chim. Acta* **2004**, *357*, 746–754. (c) Zhang, X.; Zuo, Z.; Tang, J.; Wang, K.; Wang, C.; Chen, W.; Li, C.; Xu, W.; Xiong, X.; Yuntai, K.; Huang, J.; Lan, X.; Zhou, H. B. Design, synthesis and biological evaluation of novel estrogen-derived steroid metal complexes. *Bioorg. Med. Chem. Lett*. **2013**, *23*, 3793-3707. (d) McGuirk, C. M.; Mendez-Arroyo, J.; Lifschitz; A. M.; Mirkin C. A. Allosteric regulation of supramolecular oligomerization and catalytic activity via coordination-based control of competitive hydrogen-bonding events. *J. Am. Chem. Soc*. **2014**, *136*, 16594-16601. (e) Ambrosi, G.; Formica, M.; Fusi, V.; Giorgi, L. Guerri, A.; Micheloni, M.; Paoli, P.; Pontellini, R.; Rossi, P. A New macrocyclic cryptandwith squaramide moieties: an overstructured Cu(II) complex that selectively binds halides: synthesis, acid/base- and ligational behavior, and crystal structures. *Chem. Eur. J.* **2007**, *13*, 702- 712. (f) For other metals than Pt(II) direct coordinated to squaramide motif see: López, K. A.; Piña, M. N.; Quiñonero, D.; Ballester,

P.; Morey, J.; Highly efficient coordination of $Hg^{2+}$ and $Pb^{2+}$ metals in water with squaramide-coated $Fe_3O_4$ nanoparticles. *J. Mater. Chem. A* **2014**, *2*, 8796- 8803.

(11) Chen, H.; Li, S.; Yao, Y.; Zhou, L.; Zhao, J.; Gu, Y.; Wang, K.; Li, X. Design, synthesis, and anti-tumor activities of novel triphenylethylene–coumarin hybrids, and their interactions with Ct-DNA. *Bioorg. Med. Chem. Lett.* **2013**, *23*, 4785-4789.

(12) (a) Messori, L.; Orioli, P.; Tempi, C.; Marcon, G. Interactions of selected gold(III) complexes with calf thymus DNA. *Biochem. Biophys. Res. Commun.* **2001**, *281*, 352-360. (b) Shahabadi, N.; Nemati, L. DNA Interaction studies of a platinum(II) complex containing l-histidine and 1,10-phenanthroline ligands. *DNA Cell Biol.* **2012**, *31*, 883- 890.

(13) Shahsavani, M. B.; Ahmadi, S.; Aseman, M. D.; Nabavizadeh, S. M.; Rashidi, M.; Asadi, Z.; Efrani, N.; Ghasemi, A.; Saboury, A. A.; Niazi, A.; Bahaoddini, A.; Yousefi, R. Anticancer activity assessment of two novel binuclear platinum (II) complexes. *J. Photochem. Photobiol.* **2016**, *161*, 345-354.

(14) a) Xu, Z.; Zhao, J.; Gou, S.; Xu, G. Novel hypoxia-targeting Pt(IV) prodrugs. *Chem. Commun.* **2017**, *53*, 3749-3752. b) Wilson, W. R.; Hay, M. P. Targeting hypoxia in cancer therapy *Nat. Rev. Cancer* **2011**, *11*, 393-410.

(15) The structure was also confirmed by ^{1}H NMR of commercially available 3-(methylthio)propan-1-amine in acidic conditions.

(16) Crystallographic data for this compound are compiled in the SI.

(17) Anderson, E. D.; Gorka, A. P.; Schnermann, M. J. Near-infrared uncaging or photosensitizing dictated by oxygen tension**.** *Nat. Commun.* **2016**, *7*, 13378-13386.

(18) Al-Allaf, T. A. K.; Rashan, L. J.; Steinborn, D.; Merzweiler, K.; Wagner, C. Platinum(II) and palladium(II) complexes analogous to oxaliplatin with diferent cyclohexyldicarboxylate isomeric anions and their in vitro antitumour activity. Structural elucidation of [Pt(C$_2$O$_4$)(*cis*-dach)]. *Transit. Metal Chem*. **2003**, *28*, 717- 721.

(19) Moon, J.; Kim, J.; Ahn, Y.; Shibamoto, T. Analysis and anti-helicobacter activity of sulforaphane and related compounds present in broccoli (brassica oleracea l.) sprouts. *J. Agric. Food Chem.* **2010**, *58*, 6672-6677.

(20) Bruker Apex2, Bruker AXS Inc., Madison, Wisconsin, USA, 2004.

(21) Sheldrick, G. M. SADABS, Program for empirical adsorption correction, Institute for Inorganic Chemistry, University of Göttingen, Germany, 1996.

(22) Altomare, A.; Burla, M. C.; Camilla, M.; Cascarano, G. L.; Giacovazzo, C.; Guagliardi, A.; Moliterni, A. G. G.; Polidori, G.; Spagna, R. SIR97: a new tool for crystal structure determination and refinement. *J. Appl. Cryst*. **1999**, *32*, 115-119.

(23) (a) Sheldrick, G. M. SHELX-2014, Program for crystal structure refinement, University of Göttingen, Göttingen, Germany, 2014. (b) Farrugia, L. J. WinGX suite for small-molecule single-crystal crystallography. *J. Appl. Cryst*. **1999**, *32*, 837-838.
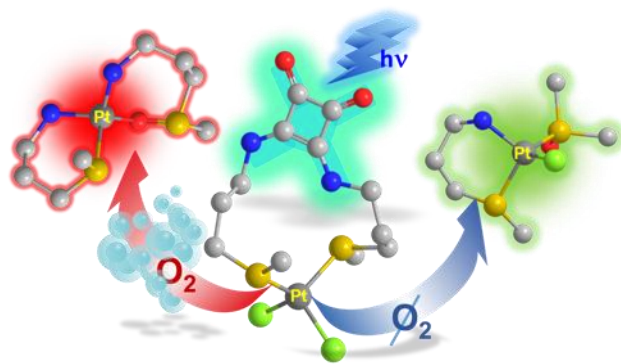
For Table of Contents Only

Synopsis

Two new squaramide-based platinum(II) complexes have been synthesized and fully characterized. Their photoresponse has been assessed and is discussed. A remarkable enhancement in the DNA binding activity has been observed for both complexes, as a result of their irradiation. The response of one of them has been found to be regulated by the presence of oxygen. In vitro cytotoxicity tests show an enhancement in its activity after irradiation selectively under hypoxic conditions.